Mendeleev Communications

Mendeleev Commun., 2025, **35**, 399–403

Random polymer formation in copolymerization of L-lactide and ε-caprolactone initiated by aluminum pyridine-bis(phenolate): a quantum chemical study

Maxim V. Zabalov,[a,b] **Badma N. Mankaev,**[b,c] **Mikhail P. Egorov**[b] **and Sergey S. Karlov***[b,c]

[a] *N. N. Semenov Federal Research Center for Chemical Physics, Russian Academy of Sciences, 119991 Moscow, Russian Federation*
[b] *N. D. Zelinsky Institute of Organic Chemistry, Russian Academy of Sciences, 119991 Moscow, Russian Federation*
[c] *Department of Chemistry, M. V. Lomonosov Moscow State University, 119991 Moscow, Russian Federation. E-mail: s.s.karlov@chemistry.msu.ru*

DOI: 10.71267/mencom.7685

The ring-opening homo- and copolymerization of ε-caprolactone (CL) and L-lactide (LA) using an aluminum complex with 2,2′-di-*tert*-butyl-6,6′-(pyridine-2,6-diyl)diphenolate and methoxide ligands as initiator was investigated by means of density functional theory (DFT) calculations. The initial stages of CL and LA polymerization as well as the first propagation stages were analyzed in detail and the activation barriers of the reactions were compared. The lowest activation barriers were found for the alternate addition of monomers, which resulted in the formation of a random copolymer as a product.

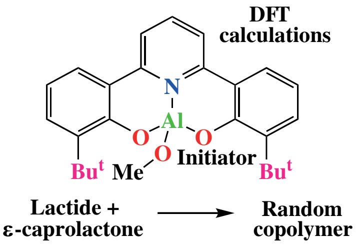

Keywords: ring-opening polymerization, copolymerization, aluminum complexes, L-lactide, biodegradable polymers, ε-caprolactone, DFT calculations, initiators.

In recent decades, biodegradable polymeric materials have attracted increasing attention. The most promising area for the use of biodegradable polymers is biomedical applications, including suture material, tissue engineering and drug delivery.[1,2] Among the various types of biodegradable polymers, polymers of cyclic esters such as caprolactone and lactide are of greatest interest due to their relative cheapness and availability.[3–8] Ring-opening polymerization (ROP) in the presence of metal complex catalyst is the best way to prepare not only homopolymers but also their copolymers,[9] and copolymerization allows obtaining materials with improved properties.[10,11] It is important to control the distribution of units in the copolymerization product and it is most desirable to obtain a random copolymer. In this way, difficulties arise due to the difference in the reaction rates of the monomers.[11,12] Depending on the type of catalyst, block, gradient and random copolymers can be formed.[13] Controlling the distribution of units in a copolymer by modifying the initiator is not easy, since it is affected by a whole complex of factors, such as the coordination properties of the metal atom, rigidity and strain in the ligand structure, donor properties of heteroatoms forming dative bonds with the metal atom, electronegativity and steric volume of substituents in the ligand. Among the catalysts, aluminum complexes are of greatest interest, since they are biocompatible and non-toxic, but often do not have high activity.[12,14–17] One of the most important biodegradable copolymers is the copolymer of L-lactide (LA) and ε-caprolactone (CL). Interestingly, homopolymers LA and CL have contrasting physical and thermal properties: poly(ε-caprolactone) exhibits good elasticity and permeability, but poor mechanical characteristics (toughness), which is opposite to the properties of poly(lactide).[18]

Although the mechanism of ROP has been studied extensively by quantum chemistry methods,[19–23] there are only a few computational studies devoted to the copolymerization of LA and CL using metal-based initiators.[24–29] Chandanabodhi and Nanok studied the mechanism of LA and CL copolymerization initiated by aluminum alkoxide complexes with salen-type ligands.[24] They found that the different reactivity observed in homo- and copolymerization of the two types of monomers was related to the binding affinities of the monomers with the initiators. Nifantiev *et al.* studied the copolymerization of LA and CL catalyzed by magnesium, aluminum and zinc complexes with 2,6-di-*tert*-butyl-4-methylphenoxy substituents.[25,26] The authors noted that the formation of a highly stable chelate product of LA ring opening is a key factor in controlling the process. We also investigated the mechanism of LA and CL copolymerization using aluminum and gallium amino-bis(phenolates) as initiators.[27,28] However, the complexes studied turned out to yield a block copolymer as a product, rather than a random copolymer as desired.

More recently, Wongnongwa *et al.* studied the mechanism of homo- and copolymerization of LA and CL catalyzed by aluminum complexes bearing amino-bis(phenolate) ligands with pyridine and diethylamine sidearms.[29] The authors found that, depending on the amine sidearm and the degree of van der Waals (vdW) interactions between the monomers and the catalysts, tapered or random products can be formed during the copolymerization process. Although their calculations are supported by experimental observations, we disagree with the authors' conclusions because there are questions regarding their method for calculating the activation barriers of key stages (see below).

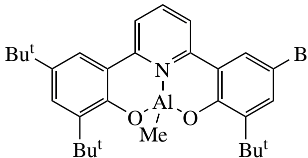

1

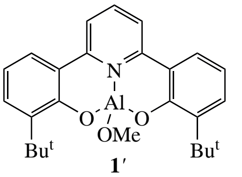

1′

We have just found that compound **1**, based on a substituted 2,6-bis(2-hydroxyphenyl)pyridine ligand, is an effective initiator of the CL and LA copolymerization, leading to the formation of the statistical copolymer poly(LA-*stat*-CL).[30] To establish the reasons for this behavior of the new initiator, in this work we investigated the catalysis mechanism of the LA and CL copolymerization using the DFT (PBE-D4/TZ2P) method. As an initiator, a closely related methoxy complex **1′** was considered, in which the Bu^t substituents at positions 5 in the phenyl rings of the ligand were replaced by hydrogen atoms in order to simplify calculations. The details of quantum chemical calculations are described in Online Supplementary Materials.

In the coordination–insertion mechanism, the metal atom is involved in the transfer of the alkoxy group to the carbonyl carbon atom of the monomer, which leads to ring opening of the monomer and the formation of a new alkoxy group bound to the metal atom. This results in the sequential growth of the polymer chain. According to our calculations, the general scheme of the coordination–insertion mechanism involving pyridine-bis(phenolate) aluminum complex **1′** is the same for both the initiation and propagation stages (Figure 1). In addition, the energy profiles of the initiation stage (Figure S1, see Online Supplementary Material) and the most important structures of the conformers corresponding to the minimum energy transition

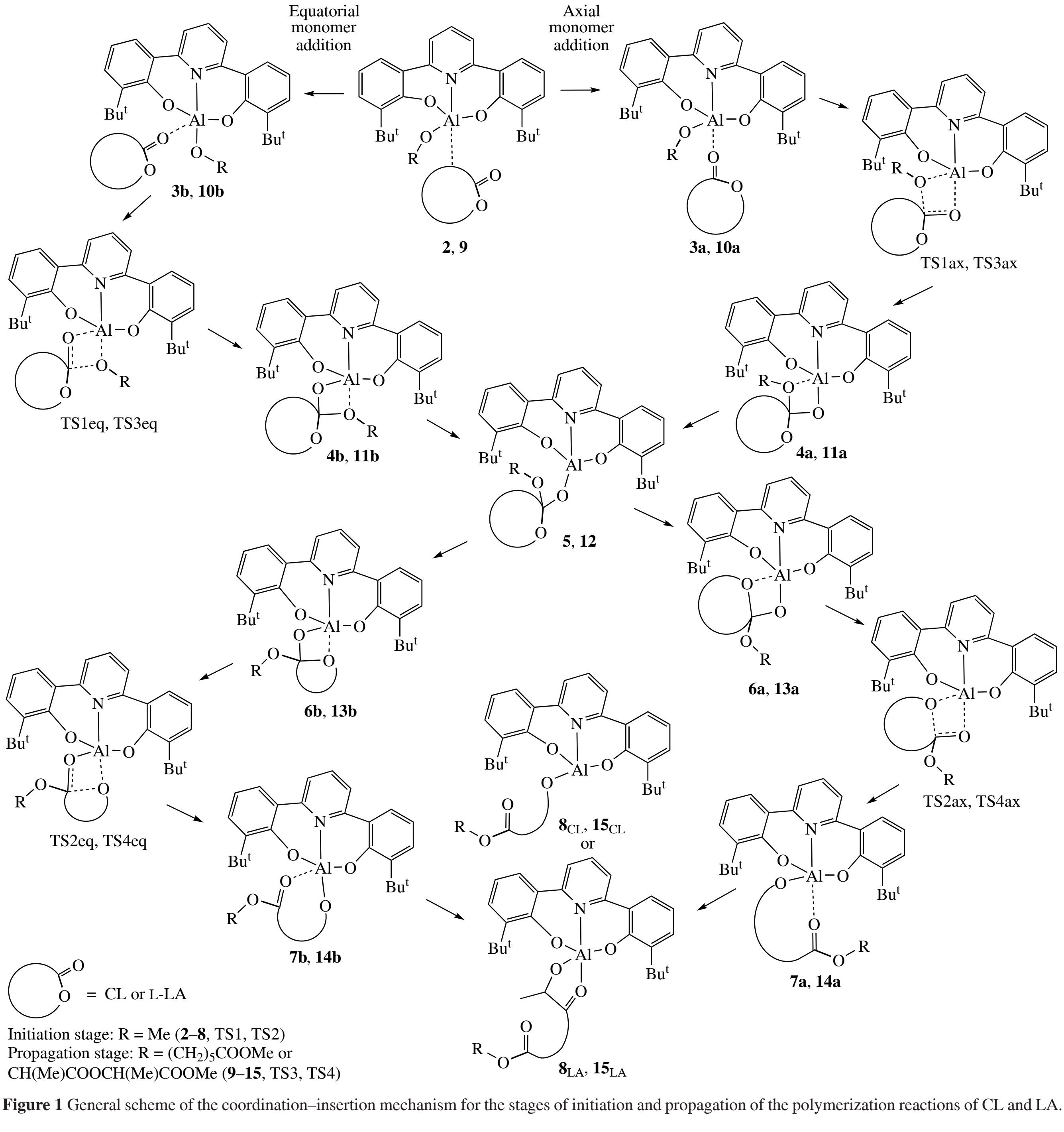

= CL or L-LA

Initiation stage: R = Me (**2**–**8**, TS1, TS2)
Propagation stage: R = $(CH_2)_5COOMe$ or
CH(Me)COOCH(Me)COOMe (**9**–**15**, TS3, TS4)

Figure 1 General scheme of the coordination–insertion mechanism for the stages of initiation and propagation of the polymerization reactions of CL and LA.

states and intermediates in the initiation stage (Figure S2) were calculated.

A detailed description of the mechanism is given in our previous articles.[27,28] Both axial and equatorial addition of monomers LA and CL to initiator **1**′ is possible. The initiator does not form stable complexes with the coordinated monomers, they are formed only as intermediates **3a**,**b** along the reaction paths. The potential energy surface at this location is very flat, and the energy barriers for transitions from intermediates **3a**,**b** to complexes **2** are less than 1 kcal mol^{-1}. Therefore, the reactions start with the formation of weak vdW complexes **2** between the reactants. The formation energies of the reactant complexes and their structures are presented in Figure S3. The same situation with low transition barriers occurs for intermediates **4**/**5**/**6** and **7**/**8** and their analogues **11**/**12**/**13** and **14**/**15** at the propagation stage.

The rate-limiting step is the transfer of the alkoxy group from the metal atom to the carbonyl carbon atom of the monomer through the four-membered cyclic TS1ax (axial path) or TS1eq (equatorial path). The lowest Gibbs free energy of activation (9.1 kcal mol^{-1}) is found in the axial reaction path for LA, the equatorial path for LA has a barrier value only 1.3 kcal mol^{-1} higher than the axial path (see Figure S1). Both the equatorial and axial reaction paths for CL have higher barriers (11.0 and 13.4 kcal mol^{-1}, respectively). As a result, it can be considered that the initiation stage starts mainly with the reaction of LA, although CL obviously reacts as well, since the difference in Gibbs free energies of activation is not large. It should be noted that the activation barriers for the reaction with pyridine-bis(phenolate) initiator **1**′ are reduced by 1.0–3.9 and 2.6–5.1 kcal mol^{-1} compared to the previously considered amino-bis(phenolate) complexes of aluminum[27] and gallium,[28] respectively. Also, intermediates **4**–**6** are more stable in the case of the pyridine-bis(phenolate) complex.

The decrease in the difference in the activation barriers for the axial and equatorial paths is due to the greater ability of the pyridine nitrogen atom, compared to the nitrogen atom of the amino group in the amino-bis(phenolate) ligand, to bind to the metal atom due to both electronic and steric factors, which leads to a stronger bonding of the monomers to the metal in the axial position.

Note that the pyridine-bis(phenolate) ligand in initiator **1**′ has a conformation that is favorable for the formation of the transition state. Figure 2 shows the changes in the geometry of initiator **1**′ en route to the transition state by superimposing a fragment of the structure of the initial vdW complex **2** on the structures of transition states TS1ax$_{\text{LA}}$ and TS1eq$_{\text{LA}}$ for the pyridine-bis(phenolate) ligand and on those for the amino-bis(phenolate) ligand[28] in the aluminum complexes.

The height of the activation barriers in transition states TS1 and their analogs corresponds to the magnitude of the change in the bond angles of the ligands in the equatorial plane relative to the initial structures of the vdW complex **2** and its analog, respectively. The complex with the amino-bis(phenolate) ligand requires a greater rearrangement of the coordination sphere around the metal for the polymerization reaction to occur and, accordingly, to overcome a higher activation barrier.

The superimposed structures of the four-membered cycles in the transition states for the pyridine-bis(phenolate) (TS1ax and TS1eq) and amino-bis(phenolate) ligands were also compared (Figure S4). For the axial addition of LA, the structures of the four-membered cycle in TS1 are almost identical and, therefore, the transition state energy is determined mainly by the change in the ligand structure. For the equatorial addition, a noticeable difference is observed in that the carbonyl group in the transition state with the amino-bis(phenolate) ligand is located further from the metal atom and the transition state corresponds to the act of the monomer approach. For the reaction with the pyridine-bis(phenolate) initiator, structure TS1 corresponds to the redistribution of bonds in the four-membered –Al–O–C–O– cycle.

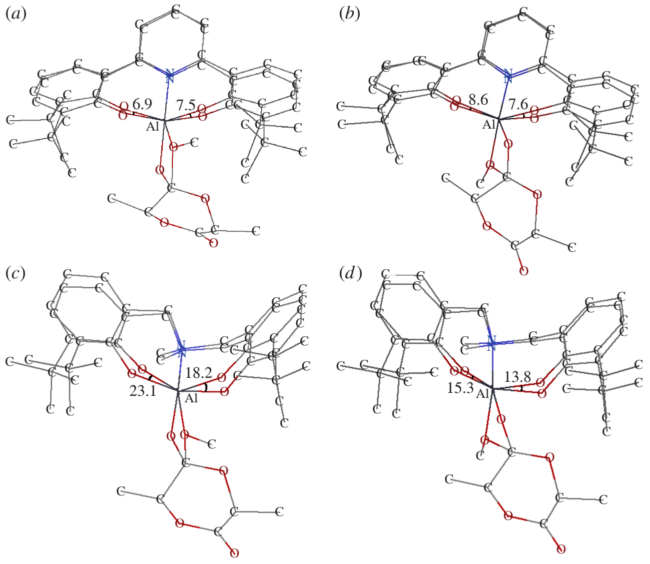

Figure 2 Geometry changes of aluminum-based LA polymerization initiators containing (*a*), (*b*) pyridine-bis(phenolate) ligand and (*c*), (*d*) amino-bis(phenolate) ligand upon formation of transition states for (*a*), (*c*) axial and (*b*), (*d*) equatorial addition of LA monomer. After alignment in the Al–N–C atoms plane, the fragment of structure **2** without LA and methoxy moieties was superimposed on the structures of (*a*) TS1ax$_{\text{LA}}$ and (*b*) TS1eq$_{\text{LA}}$, as well as on their corresponding (*c*) axial and (*d*) equatorial analogs with the amino ligand. The corresponding Gibbs free energies of activation were calculated as (*a*) 9.1, (*b*) 10.4, (*c*) 16.3 and (*d*) 13.0 kcal mol^{-1}.

The product of the initiation stage involving CL or LA is either the ring-opened complex **8**$_{\text{CL}}$ or the chelate complex **8**$_{\text{LA}}$, respectively (see Figures 1 and S1). The formation of the chelate intermediate is a distinctive feature of the LA reaction, and this fundamentally affects the energetics of the subsequent chain growth stages,[19,20,24,27,28] since the high stability of complex **8**$_{\text{LA}}$ leads to the need to overcome higher barriers in the next polymerization stage. The formation of two types of chelates with axial and equatorial arrangement of the carbonyl O atom is possible, with the axial complex being more favorable and having a lower energy by 5.4 kcal mol^{-1}.

Thus, both monomers can react at the initiation stage, but LA is more likely to react. The energy barriers for the axial and equatorial reaction paths are very close, and competition between the paths is possible.

The propagation stage is the most important in the polymerization reaction and follows the same mechanism as the initiation stage (see Figure 1). The only difference is in the stability of the initial intermediate **9**, from which the activation energy barrier of the transition state TS3 at the rate-limiting stage is calculated. At the initiation stage, the stabilities of the vdW complexes **2**$_{\text{CL}}$ and **2**$_{\text{LA}}$ are approximately the same. At the propagation stage, after the addition of LA, the very stable chelate **8**$_{\text{LA}}$ is formed, and for the reaction to proceed through TS3, a higher barrier must be overcome in this case. The role of chelate intermediates has also been noted in the works of other authors.[24–27,29,31–34] It was found that the stability of chelates is mainly influenced by the electronegativity of substituents in the ligand and the type of metal atom in the complex.[24–26,33]

Recently, Wongnongwa *et al.* investigated the mechanism of homo- and copolymerization of LA and CL initiated by two aluminum complexes differing in the ligand sidearms. The authors, using the DFT method, found that variation of the amine sidearms and the vdW interactions of the monomers with the catalysts led to the formation of different copolymer products, tapered and random copolymers.[29]

Having analyzed their results, we realized that the authors' conclusions are not reliable, since they are based on a comparison of the activation barriers for the rate-limiting stages calculated relative to the nearest local minima preceding the transition state on the reaction coordinate [ref. 29, Figures 7(*b*) and 8(*b*), structure TS3]. It is correct to calculate the reaction barriers from the ground state corresponding to the global minimum for each reaction stage. At the propagation stage, the ground state is the vdW complex of the monomer with the initiator chelate complex formed as a result of the addition of LA at the initiation stage, or with the initiator carrying the free tail of the opened monomer residue formed as a result of the addition of CL at the initiation stage. Although the products of the initiation stages were always ground states [ref. 29, Figures 7(*b*) and 8(*b*), structure Int3], the authors used the energies of less stable complexes, namely, complexes of monomers coordinated by the carbonyl oxygen atom to the aluminum atom of the initiator, as reference levels for calculating the activation barriers. Such complexes do not always correspond to the ground state, and in the case of the propagation stage after the addition of LA, they always lie higher in energy than the vdW complexes of the chelate with the monomers. We estimated the energy barriers for the propagation stages of CL and LA copolymerization and found that for the two catalysts, regardless of the sidearm, it is advantageous to add CL after the addition of both CL and LA. That is, there is no difference between the two catalysts with different sidearms, and a tapered copolymer must be formed with both.

According to the experimental data,[35] the copolymerization of CL and LA is clearly dominated by the CL polymerization reaction. Although this dominance is small for the catalyst with a pyridine sidearm and the reaction behavior looks like the formation of a random copolymer, it should be noted that such behavior is characteristic only for harsh reaction conditions (temperature 100 °C). At 70 °C, the polymerization of LA is significantly slower than the polymerization of CL and occurs only when catalyzed by the complex with a pyridine sidearm.[34] At 20 °C, LA blocks the reaction and it stops completely.[36] The reaction can be resumed only when heated again to 100 °C. At such a high temperature (100 °C), the difference in the reactions barriers ceases to be a determining factor, since both energy barriers can be overcome. However, some advantage of the reaction with a lower barrier is manifested in the experimental data as a slightly higher conversion of CL during the copolymerization reaction.[35]

In the case of copolymerization using the pyridine-bis(phenolate) aluminum initiator considered in this work, the situation with the activation barriers is different from everything discussed previously. A stable chelate is also formed after the addition of LA, which leads to an increase in the activation barriers for the next stage of addition of any monomer (Figure 3) and a slowing down of the reaction at this stage. However, our calculated data have shown for the first time that at the next step after the addition of LA, the activation barrier for the addition of CL *via* TS3ax$_{\mathrm{LACL}}$ or TS3eq$_{\mathrm{LACL}}$ is 2.8 kcal mol^{-1} lower than for the addition of LA *via* TS3ax$_{\mathrm{LALA}}$. In contrast, after the addition of CL, the activation barrier for the subsequent addition of LA *via* TS3ax$_{\mathrm{CLLA}}$ is 3.8 kcal mol^{-1} lower (see Figure 3) than for the addition of CL *via* TS3eq$_{\mathrm{CLCL}}$. As a result, it is not advantageous to form chains of identical monomer units, such as –CL–CL– or –LA–LA–, but it is advantageous to alternate units and form a copolymer with a predominantly random distribution of units. The characteristic structures of the transition states and intermediates for the most profitable paths of the propagation stages and the Gibbs free energy profiles of all possible paths are presented in Figures S5–S7.

The differences in the TS3 structures for different monomers and initiators are not as obvious as they were in TS1. Due to the more complex structure, additional factors interfere, such as, for example, the orientation of the CL or LA open monomer tail relative to the ligand. Conformational analysis of intermediate **8**$_{\mathrm{CL}}$ showed that a change in the conformation and position of the open monomer tail relative to the ligand can lead to a difference in the energy of the intermediate structures of 17.5 kcal mol^{-1}. Thus, the distribution of monomer units in the copolymer is

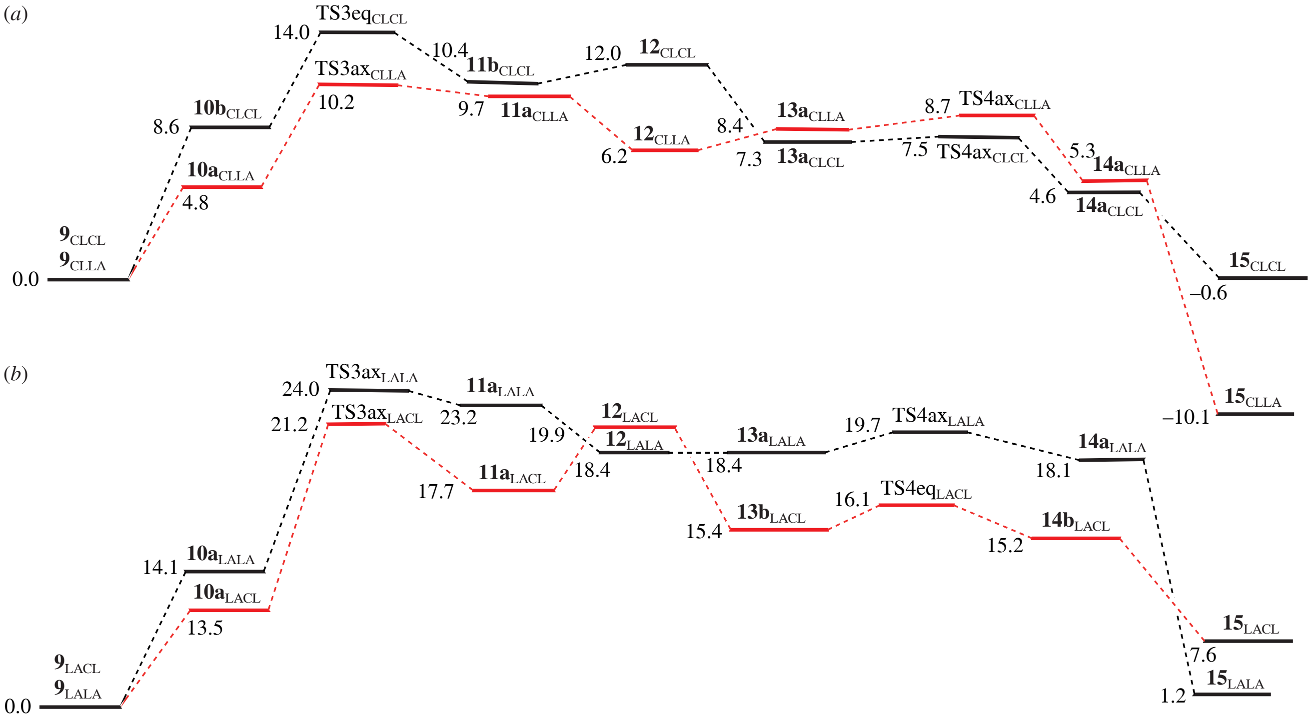

Figure 3 Relative Gibbs free energy profiles (in kcal mol^{-1}) of the competitive paths for the addition of CL and LA at the propagation stage following the addition of (*a*) CL or (*b*) LA at the initiation stage. The red line shows the most favorable reaction path.

influenced by a combination of factors, and in the presence of aluminum pyridine-bis(phenolate), it is advantageous to alternate units due to the lowest barriers for the corresponding reactions.

In addition to steric hindrances in the ligands and the presence of electronegative substituents in them, the distribution of units in the copolymer is also affected by the structural strain in the initiator, which determines the degree of adjustment of the complex structure in the transition state, as well as the donor ability of the ligands, which determines the stability of the transition states. For example, the donor ability of pyridine is higher than that of a tertiary amine, which in our case, along with other factors, contributed to the formation of a copolymer with a random distribution of units. The results obtained in this work are confirmed by experimental studies of the structure of the copolymer obtained by copolymerization of CL and LA, catalyzed by pyridine-bis(phenolate) aluminum complex **1**.[30]

In conclusion, the initiation and first propagation stages of the pyridine-bis(phenolate) aluminum initiator-mediated copolymerization of LA and CL were investigated using the DFT method. It was found that LA is more likely to react first at the initiation stage. The small difference in the activation barriers between the axial and equatorial reaction paths leads to their competition and a greater diversity of reaction paths. The rigidity of the pyridine-bis(phenolate) ligand and the donor ability of pyridine lead to the formation of an initiator structure favorable for the reaction, which in turn leads to a decrease in the activation barriers along all paths.

When LA is added to the polymer chain, a stable chelate complex is formed, which leads to an increase in the activation barriers of the next stage of addition of any monomer and requires a higher temperature for the copolymerization reaction to occur. An important feature of the mechanism of copolymerization of LA and CL, established for the first time, is that after the addition of LA, the activation barrier is lower for the subsequent reaction with CL, and after the addition of CL, the activation barrier is lower for the subsequent reaction with LA, as a result of which a polymer with a random distribution of units is formed.

This work was supported by the Russian Science Foundation (grant no. 20-13-00391).

Online Supplementary Materials

Supplementary data associated with this article can be found in the online version at doi: 10.71267/mencom.7685.

References

1 D. K. Schneiderman and M. A. Hillmyer, *Macromolecules*, 2017, **50**, 3733; https://doi.org/10.1021/acs.macromol.7b00293.

2 A. Samir, F. H. Ashour, A. A. A. Hakim and M. Bassyouni, *npj Mater. Degrad.*, 2022, **6**, 68; https://doi.org/10.1038/s41529-022-00277-7.

3 Č. Maja, K.-H. Maša, Š. Mojca and K. Željko, *Chem. Ind. Chem. Eng. Q.*, 2020, **26**, 401; https://doi.org/10.2298/CICEQ191210018C.

4 E. T. H. Vink, K. R. Rábago, D. A. Glassner and P. R. Gruber, *Polym. Degrad. Stab.*, 2003, **80**, 403; https://doi.org/10.1016/S0141-3910(02)00372-5.

5 A. P. Gupta and V. Kumar, *Eur. Polym. J.*, 2007, **43**, 4053; https://doi.org/10.1016/j.eurpolymj.2007.06.045.

6 K. Yao and C. Tang, *Macromolecules*, 2013, **46**, 1689; https://doi.org/10.1021/ma3019574.

7 S. O. Alaswad, A. S. Mahmoud and P. Arunachalam, *Polymers*, 2022, **14**, 4924; https://doi.org/10.3390/polym14224924.

8 G. Satchanska, S. Davidova and P. D. Petrov, *Polymers*, 2024, **16** 1159; https://doi.org/10.3390/polym16081159.

9 B. N. Mankaev and S. S. Karlov, *Materials*, 2023, **16**, 6682; https://doi.org/10.3390/ma16206682.

10 R. M. Rasal, A. V. Janorkar and D. E. Hirt, *Prog. Polym. Sci.*, 2010, **35**, 338; https://doi.org/10.1016/j.progpolymsci.2009.12.003.

11 E. Stirling, Y. Champouret and M. Visseaux, *Polym. Chem.*, 2018, **9**, 2517; https://doi.org/10.1039/C8PY00310F.

12 N. Nomura, A. Akita, R. Ishii and M. Mizuno, *J. Am. Chem. Soc.*, 2010, **132**, 1750; https://doi.org/10.1021/ja9089395.

13 O. Dechy-Cabaret, B. Martin-Vaca and D. Bourissou, *Chem. Rev.*, 2004, **104**, 6147; https://doi.org/10.1021/cr040002s.

14 C. Kan and H. Ma, *RSC Adv.*, 2016, **6**, 47402; https://doi.org/10.1039/C6RA07374C.

15 T. Shi, W. Luo, S. Liu and Z. Li, *J. Polym. Sci., Part A: Polym. Chem.*, 2018, **56**, 611; https://doi.org/10.1002/pola.28932.

16 G. Li, M. Lamberti, D. Pappalardo and C. Pellecchia, *Macromolecules*, 2012, **45**, 8614; https://doi.org/10.1021/ma3019848.

17 R. H. Platel, L. M. Hodgson and C. K. Williams, *Polym. Rev.*, 2008, **48**, 11; https://doi.org/10.1080/15583720701834166.

18 A. Arbaoui and C. Redshaw, *Polym. Chem.*, 2010, **1**, 801; https://doi.org/10.1039/B9PY00334G.

19 I. Nifant'ev and P. Ivchenko, *Molecules*, 2019, **24**, 4117; https://doi.org/10.3390/molecules24224117.

20 I. Nifant'ev and P. Ivchenko, *Polymers*, 2019, **11**, 2078; https://doi.org/10.3390/polym11122078.

21 Y.-L. Hsieh, W. Benchaphanthawee, H.-H. Teng, N. Huang, J.-H. Yang, J.-R. Sun, G.-H. Lee, N. Kungwan and C.-H. Peng, *Polymer*, 2023, **267**, 125687; https://doi.org/10.1016/j.polymer.2023.125687.

22 Y. Rusconi, M. C. D'Alterio, A. Grillo, A. Poater, C. De Rosa and G. Talarico, *Polymer*, 2024, **292**, 126639; https://doi.org/10.1016/j.polymer.2023.126639.

23 Y. Rusconi, M. C. D'Alterio, C. De Rosa, Y. Lu, S. M. Severson, G. W. Coates and G. Talarico, *ACS Catal.*, 2024, **14**, 318; https://doi.org/10.1021/acscatal.3c04955.

24 D. Chandanabodhi and T. Nanok, *Mol. Catal.*, 2017, **436**, 145; https://doi.org/10.1016/j.mcat.2017.04.005.

25 I. Nifant'ev, A. Shlyakhtin, M. Kosarev, D. Gavrilov, S. Karchevsky and P. Ivchenko, *Polymers*, 2019, **11**, 1641; https://doi.org/10.3390/polym11101641.

26 I. Nifant'ev, P. Komarov, V. Ovchinnikova, A. Kiselev, M. Minyaev and P. Ivchenko, *Polymers*, 2020, **12**, 2273; https://doi.org/10.3390/polym12102273.

27 M. V. Zabalov, B. N. Mankaev, M. P. Egorov and S. S. Karlov, *Int. J. Mol. Sci.*, 2022, **23**, 15523; https://doi.org/10.3390/ijms232415523.

28 M. V. Zabalov, B. N. Mankaev, M. P. Egorov and S. S. Karlov, *Russ. Chem. Bull.*, 2023, **72**, 602; https://doi.org/10.1007/s11172-023-3824-6.

29 Y. Wongnongwa, S. Haesuwannakij, K. Udomsasporn, P. Chumsaeng, A. Watcharapasorn, K. Phomphrai and S. Jungsuttiwong, *Polymer*, 2023, **281**, 126065; https://doi.org/10.1016/j.polymer.2023.126065.

30 B. N. Mankaev, V. A. Serova, M. U. Agaeva, K. A. Lyssenko, A. N. Fakhrutdinov, A. V. Churakov, E. V. Chernikova, M. P. Egorov and S. S. Karlov, *J. Organomet. Chem.*, 2024, **1005**, 122973; https://doi.org/10.1016/j.jorganchem.2023.122973.

31 S. Tabthong, T. Nanok, P. Sumrit, P. Kongsaeree, S. Prabpai, P. Chuawong and P. Hormnirun, *Macromolecules*, 2015, **48**, 6846; https://doi.org/10.1021/acs.macromol.5b01381.

32 J. Lewiński, P. Horeglad, K. Wójcik and I. Justyniak, *Organometallics*, 2005, **24**, 4588; https://doi.org/10.1021/om050295v.

33 I. E. Nifant'ev, A. V. Shlyakhtin, A. N. Tavtorkin, P. V. Ivchenko, R. S. Borisov and A. V. Churakov, *Catal. Commun.*, 2016, **87**, 106; https://doi.org/10.1016/j.catcom.2016.09.018.

34 P. Chumsaeng, S. Haesuwannakij, S. Bureekaew, V. Ervithayasuporn, S. Namuangruk and K. Phomphrai, *Inorg. Chem.*, 2018, **57**, 10170; https://doi.org/10.1021/acs.inorgchem.8b01364.

35 P. Chumsaeng, S. Haesuwannakij, A. Virachotikul and K. Phomphrai, *J. Polym. Sci., Part A: Polym. Chem.*, 2019, **57**, 1635; https://doi.org/10.1002/pola.29425.

36 K. Phomphrai, P. Chumsaeng, P. Sangtrirutnugul, P. Kongsaeree and M. Pohmakotr, *Dalton Trans.*, 2010, **39**, 1865; https://doi.org/10.1039/B919340E.

Received: 15th November 2024; Com. 24/7685